1521-0111/12/8204-591–600$25.00
MOLECULAR PHARMACOLOGY
Vol. 82, No. 4
79004/3792439

Mol Pharmacol 82:591–600, 2012

Functional Loss of the Reduced Folate Carrier Enhances the Antitumor Activities of Novel Antifolates with Selective Uptake by the Proton-Coupled Folate Transporter[S]

Sita Kugel Desmoulin, Lei Wang, Lisa Polin, Kathryn White, Juiwanna Kushner, Mark Stout, Zhanjun Hou, Christina Cherian, Aleem Gangjee, and Larry H. Matherly

Graduate Program in Cancer Biology (S.K.D., L.H.M.) and Departments of Oncology (S.K.D., L.P., K.W., J.K., Z.H., C.C., L.H.M.) and Pharmacology (L.H.M.), Wayne State University School of Medicine, Detroit, Michigan; Molecular Therapeutics Program, Barbara Ann Karmanos Cancer Institute, Detroit, Michigan (L.P., Z.H., C.C., L.H.M.); Department of Pediatrics, Children's Hospital of Michigan, Detroit, Michigan (M.S.); and Division of Medicinal Chemistry, Graduate School of Pharmaceutical Science, Duquesne University, Pittsburgh, Pennsylvania (L.W., A.G.)

Received March 29, 2012; accepted June 26, 2012

ABSTRACT

Uptake of 6-substituted pyrrolo[2,3-*d*]pyrimidine thienoyl antifolates with four or three bridge carbons [compound **1** (**C1**) and compound **2** (**C2**), respectively] into solid tumors by the proton-coupled folate transporter (PCFT) represents a novel therapeutic strategy that harnesses the acidic tumor microenvironment. Although these compounds are not substrates for the reduced folate carrier (RFC), the major facilitative folate transporter, RFC expression may alter drug efficacies by affecting cellular tetrahydrofolate (THF) cofactor pools that can compete for polyglutamylation and/or binding to intracellular enzyme targets. Human tumor cells including wild-type (WT) and R5 (RFC-null) HeLa cells express high levels of PCFT protein. **C1** and **C2** inhibited proliferation of R5 cells 3 to 4 times more potently than WT cells or R5 cells transfected with RFC. Transport of **C1** and **C2** was virtually identical between WT and R5 cells, establishing that differences in drug sensitivities between sublines were independent of PCFT transport. Steady-state intracellular [^{3}H]THF cofactors derived from [^{3}H]5-formyl-THF were depleted in R5 cells compared with those in WT cells, an effect exacerbated by **C1** and **C2**. Whereas **C1** and **C2** polyglutamates accumulated to similar levels in WT and R5 cells, there were differences in polyglutamyl distributions in favor of the longest chain length forms. In severe combined immunodeficient mice, the antitumor efficacies of **C1** and **C2** were greater toward subcutaneous R5 tumors than toward WT tumors, confirming the collateral drug sensitivities observed in vitro. Thus, solid tumor-targeted antifolates with PCFT-selective cellular uptake should have enhanced activities toward tumors lacking RFC function, reflecting contraction of THF cofactor pools.

Introduction

Classic antifolates such as methotrexate (MTX) and pemetrexed (PMX), like folate cofactors, have minimal lipid solubility and therefore require specific transport mechanisms to enter mammalian cells. There are three primary folate transporters, including the reduced folate carrier (RFC), the proton-coupled folate transporter (PCFT), and folate receptor (FR) α (Assaraf, 2007; Goldman et al., 2010). RFC is the predominant transport route for the major circulating folate, 5-methyl tetrahydrofolate (THF), and (6*S*)-5-formyl THF (5-CHO-THF) in mammalian cells and tissues (Matherly et al., 2007). RFC also mediates cellular uptake of MTX and is essential to MTX antitumor activity (Matherly et al., 2007). Impaired RFC function is a major mechanism of MTX resistance in cultured tumor cells selected in vitro (Zhao and Goldman, 2003; Matherly et al., 2007) and in murine leuke-

This study was supported by the National Institutes of Health National Cancer Institute [Grants CA53535, CA152316, CA125153]; the Barbara Ann Karmanos Cancer Institute; and the Mesothelioma Applied Research Foundation. S.K.D. was supported by a Doctoral Research Award from the Canadian Institute of Health Research.

A.G. and L.H.M. contributed equally to this work.

Article, publication date, and citation information can be found at http://molpharm.aspetjournals.org.
http://dx.doi.org/10.1124/mol.112.079004.

[S] The online version of this article (available at http://molpharm.aspetjournals.org) contains supplemental material.

ABBREVIATIONS: MTX, methotrexate; PMX, pemetrexed; RFC, reduced folate carrier; PCFT, proton-coupled folate transporter; FR, folate receptor; THF, tetrahydrofolate; 5-CHO-THF, 5-formyl-tetrahydrofolate; **C1**, compound **1; C2**, compound **2;** hRFC, human reduced folate carrier; hPCFT, human proton-coupled folate transporter; HA, hemagglutinin; WT, wild-type; RT, reverse transcription; PCR, polymerase chain reaction; MES, 4-morphilinopropane sulfonic acid; DPBS, Dulbecco's phosphate-buffered saline; PIPES, piperazine-*N*,*N*′-bis(2-ethanesulfonic acid); HPLC, high-performance liquid chromatography; SCID, severe combined immunodeficient; LMX, lometrexol; RTX, raltitrexed; PT523, N^{α}-(4-amino-4-deoxypteroyl)-N^{δ}-hemiphthaloyl-L-ornithine; PG, polyglutamate; FPGS, folylpolyglutamate synthetase; ABC, ATP-binding cassette.

mia cells in vivo (Sirotnak et al., 1981). Loss of RFC function in clinical specimens has also been reported (Gorlick et al., 1997; Guo et al., 1999; Yang et al., 2003). RFC transport of cytotoxic antifolates can also be undesirable because RFC is ubiquitously expressed and exhibits a high level of activity at the neutral pH values characterizing most normal tissues (Matherly et al., 2007). Thus, transport of antifolates by RFC could easily preclude tumor selectivity and cause toxicity to normal tissues.

The novel 6-substituted pyrrolo[2,3-*d*]pyrimidine thienoyl antifolates with four [compound **1** (**C1**)] or three [compound **2** (**C2**)] carbon bridge lengths (Fig. 2A) represent a new class of antitumor agents that exhibit a lack of significant membrane transport by RFC (Wang et al., 2010, 2011; Kugel Desmoulin et al., 2011). Cellular uptake of **C1** and **C2** by PCFT and FRα is efficient and offers a promising new strategy for solid tumor targeting (Anderson and Thwaites, 2010; Kugel Desmoulin et al., 2011). Because PCFT functions optimally at acidic pH values (Qiu et al., 2006; Umapathy et al., 2007; Zhao et al., 2008), transport of **C1** and **C2** by PCFT may lead to further enhancement of tumor selectivity owing to the acidic microenvironments of many solid tumors (Helmlinger et al., 1997; Gillies et al., 2002; Anderson and Thwaites, 2010; Webb et al., 2011). Our previous results established that **C1** and **C2** are potent inhibitors of tumor cell proliferation both in vitro and in vivo (Wang et al., 2010, 2011; Kugel Desmoulin et al., 2011).

For agents such as PMX that are excellent substrates for both RFC and PCFT, loss of RFC has a limited effect on overall activity, because PMX uptake is maintained by PCFT (Zhao et al., 2004c, 2008). Paradoxically, RFC loss has been shown to enhance antitumor activity (i.e., collateral sensitivity) of PMX via decreased intracellular THF cofactor pools (Zhao et al., 2004c; Chattopadhyay et al., 2006, 2007). This response to RFC loss can be further affected by the type and amount of extracellular folate (Zhao et al., 2004b,c; Chattopadhyay et al., 2006).

An analogous effect may exist for PCFT-selective substrates such as **C1** and **C2**, although this has never been systematically tested. In this report, we examine the complex interplay between RFC and extracellular reduced folates. Specifically, we investigate the mechanistic ramifications of loss of RFC function on in vitro and in vivo antitumor efficacies of these PCFT-targeted antifolates. Our results strongly imply that levels of folate transport by RFC in tumors are critical determinants of drug efficacy for this novel class of PCFT-selective antitumor agents.

Materials and Methods

Materials. [3′,5′,7-^{3}H]MTX (20 Ci/mmol), [^{3}H]PMX (2.5 Ci/mmol), [3′,5′,7,9-^{3}H(*N*)](6*S*)-5-formyl tetrahydrofolate (16.6 Ci/mmol), and custom-radiolabeled [^{3}H]**C1** (1.3 Ci/mmol) and [^{3}H]**C2** (16 Ci/mmol) were purchased from Moravek Biochemicals (Brea, CA). Sources of the nonradioactive folate and antifolate drugs are summarized in Supplemental Table 1S.

Cell Lines. The sources and cell culture conditions for assorted human solid tumor cell lines are summarized in Supplemental Table 2S. HeLa cells were obtained commercially. RFC-null R5 HeLa cells were described previously (Zhao et al., 2004b). R1-11-mock and R1-11-PCFT4 HeLa cells were derived from human RFC (hRFC)- and -null R1-11 cells by stable transfection with pZeoSV2(+) vector (Invitrogen, Carlsbad, CA) only or with hemagglutinin (HA)-tagged hPCFT in pZeoSV2(+), respectively. Characteristics and culture conditions of the engineered HeLa sublines were described previously (Zhao et al., 2008) and are also in Supplemental Table 2S.

Preparation of hRFC^{HA}/pZeoSV2 and Generation of Stable hRFC R5 Transfectants. Full-length hRFC was subcloned using BamHI and XhoI into pZeoSV2(+) in-frame with a C-terminal HA sequence to generate hRFC^{HA}/pZeoSV2. The plasmid was transformed into XL10-Gold ultracompetent cells (Agilent Technologies, Santa Clara, CA) and selected using low-salt LB agar plates containing 25 μg/ml phleomycin (Zeocin). Plasmids were isolated and the wild-type (WT) hRFC insert was confirmed by DNA sequencing by Genewiz Corp. (South Plainfield, NJ).

R5 cells were transfected with pZeoSV2 vector control or hRFC^{HA}/pZeoSV2 with Lipofectamine 2000 and Opti-MEM (Invitrogen). After 24 h, the cells were cultured with phleomycin (0.1 mg/ml). Stable clones were selected by plating for individual colonies in the presence of 0.1 mg/ml phleomycin. Colonies were isolated, expanded, and screened for expression of hRFC^{HA} by real-time reverse transcription (RT)-polymerase chain reaction (PCR), Western blotting, and transport assays at pH 7.2 (below). A representative clone (R5-RFC2) was selected for further study. R5 cells transfected with empty pZeoSV2 (R5-mock) were also prepared.

Gel Electrophoresis and Western Blotting. To characterize hPCFT and hRFC protein levels in assorted human solid tumor cell lines and the R5-RFC2 transfectant, plasma membranes were prepared by differential centrifugation and sucrose density centrifugation (Matherly et al., 1991). Proteins were quantified with the Folin phenol reagent (Lowry et al., 1951).

Membrane proteins were electrophoresed on 7.5% polyacrylamide gels with SDS (Laemmli, 1970) and electroblotted onto polyvinylidene difluoride membranes (Thermo Fisher Scientific, Waltham, MA) (Matsudaira, 1987). For detecting total immunoreactive hPCFT and hRFC proteins on polyvinylidene difluoride membranes, hPCFT- or hRFC-specific polyclonal antibodies raised in rabbits to carboxyl termini hPCFT or hRFC (Wong et al., 1998; Hou et al., 2012) peptides and an IRDye800CW-conjugated goat anti-rabbit IgG secondary antibody (Rockland Immunochemicals, Gilbertsville, PA) were used. For detecting HA-tagged proteins (i.e., R5-RFC^{HA}), HA-specific mouse monoclonal antibody (Covance Research Products, Princeton, NJ) and an IRDye800CW-conjugated goat anti-mouse IgG secondary antibody (Rockland Immunochemicals) were used. Membranes were scanned with the Odyssey infrared imaging system. hPCFT and hRFC levels were normalized to levels of Na^+/K^+-ATPase (Novus Biologicals, Inc., Littleton, CO).

Transport Assays. To assay hPCFT transport in assorted solid tumor cell lines, uptake of 0.5 μM [^{3}H]MTX was measured in cell monolayers in 60-mm dishes over 5 min at 37°C. The transport buffer was MES-buffered saline (20 mM MES, 140 mM NaCl, 5 mM KCl, 2 mM $MgCl_2$, and 5 mM glucose) at pH 5.5 (Zhao et al., 2004b). Some transport experiments were performed with 20 nM folic acid to exclude cellular uptake by FRs.

The pH-dependent uptake of [^{3}H]**C1,** [^{3}H]**C2,** [^{3}H]PMX, or [^{3}H]MTX (0.5 μM) in the HeLa sublines was assayed at 37°C in cell monolayers over 2 min at 37°C in 2 ml of "anion-free" HEPES-sucrose-Mg^{+2} buffer (20 mM HEPES and 235 mM sucrose, pH adjusted to 7.14 with MgO) (AFB) (Wong et al., 1997), HEPES-buffered saline (20 mM HEPES, 140 mM NaCl, 5 mM KCl, 2 mM $MgCl_2$, and 5 mM glucose, pH 6.8), or in MES-buffered saline, pH 5.5. Transport fluxes were stopped by aspirating the buffer and quenching with excess (>5 ml) ice-cold Dulbecco's phosphate-buffered saline (DPBS), followed by 3 washes with DPBS. Cellular proteins were solubilized with 0.5 N NaOH and quantified with the Folin phenol reagent (Lowry et al., 1951). Drug uptake was expressed as picomoles per milligram of protein, calculated from measurements of radioactivity with a scintillation counter and the protein contents of the cell homogenates.

To measure PCFT transport kinetics (K_t and V_{max}) for [^{3}H]**C2** in engineered R1-11-PCFT4 HeLa cells, cells were grown in spinner

flasks, collected by centrifugation, washed with DPBS, and suspended (at 1.5×10^7 cells) in 2 ml of MES-buffered saline at pH 5.5 containing [^{3}H]**C2** substrate concentrations ranging from 0.04 to 5 μM. K_t and V_{max} values were determined from Lineweaver-Burk plots. Kinetic constants for **C2** were compared with those previously published for R1-11-PCFT4 cells for **C1** and PMX (Kugel Desmoulin et al., 2011).

Real-Time RT-PCR Analysis of RFC, FRα, and PCFT Transcripts. RNAs were prepared from WT, R5, and R5-RFC2 HeLa cells using TRIzol reagent (Invitrogen). cDNAs were synthesized using random hexamers, RNase inhibitor, and MuLV reverse transcriptase and purified with the QIAquick PCR Purification Kit (QIAGEN, Valencia, CA). Quantitative real-time RT-PCR was performed on a Roche LightCycler 1.2 (Roche Diagnostics, Indianapolis, IN) with gene-specific primers and FastStart DNA Master SYBR Green I Reaction Mix (Roche Diagnostics) (Ge et al., 2007). Primers are listed in Supplemental Table 3S. Transcript levels for hRFC were normalized to those for glyceraldehyde-3-phosphate dehydrogenase. External standard curves were constructed for each gene of interest using serial dilutions of linearized templates, prepared by amplification from suitable cDNA templates, subcloning into a TA cloning vector (PCR-Topo; Invitrogen), and restriction digestions.

Cell Proliferation Assays. For proliferation assays, WT and the R5 HeLa sublines were cultured in folate-free RPMI 1640 medium, pH 7.2, supplemented with 10% dialyzed fetal bovine serum, 2 mM L-glutamine, and 100 units/ml penicillin/100 μg/ml streptomycin (hereafter referred to as "complete folate-free RPMI 1640 medium"), containing 25 nM 5-CHO-THF, for at least 2 weeks before the experiment. For drug inhibition assays, the cells were plated in 96-well culture dishes (2500 cells/well; 200 μl/well) in the above medium with a range of drug concentrations; cells were incubated for up to 96 h at 37°C in a CO_2 incubator. Numbers of cells were assayed with Cell Titer Blue cell viability assays (Promega, Madison, WI) with a fluorescent plate reader for determining IC_{50} values (drug concentrations that result in 50% loss of cell growth). To test the impact of extracellular folates on the collateral sensitivities of **C1** and **C2** in the HeLa sublines, some growth inhibition experiments included increasing concentrations (25, 100, and 1000 nM) of 5-CHO-THF.

Accumulation of [^{3}H]5-CHO-THF. WT and R5 HeLa sublines were cultured in complete folate-free RPMI 1640 medium supplemented with 0.06 mM adenosine and 0.01 mM thymidine for 5 days before the experiment. Adenosine and thymidine were added to circumvent folate requirements and to maintain cell viability in the absence of exogenous folates. Cells were treated with 0, 25, 100, and 1000 nM [^{3}H]5-CHO-THF (because [^{3}H](6*S*)-5-CHO-THF was diluted with nonradioactive (6*R,S*)-5-CHO-THF for these experiments, the actual concentration of (6*S*) stereoisomer was 12.5, 50, and 500 nM, respectively) for 4 days, followed by three washes with ice-cold DPBS. A control without added [^{3}H]5-CHO-THF (including 0.06 mM adenosine and 0.01 mM thymidine) was incubated in parallel. Cellular proteins were solubilized with 0.5 N NaOH and quantified using the Folin phenol reagent (Lowry et al., 1951). Total cellular [^{3}H]5-CHO-THF accumulations were expressed as picomoles per milligram of protein, calculated from direct measurements of radioactivity and protein contents of cell homogenates. Because [^{3}H](6*S*)-5-CHO-THF was diluted with unlabeled (6*R,S*)-5-CHO-THF (see above), for purposes of calculating intracellular folate metabolites only the unlabeled (6*S*) isomer was considered. To measure the impact of the PCFT-targeted therapeutics **C1** and **C2** on [^{3}H]5-CHO-THF accumulations, some experiments analyzed the uptake of 25 nM [^{3}H]5-CHO-THF in the presence of increasing concentrations (0–1000 nM) of compounds **C1** and **C2** in complete folate-free RPMI 1640 medium supplemented with 0.06 mM adenosine.

Measurement of C1 and C2 Polyglutamylation. WT and R5 HeLa cells were depleted of folates by growth for 2 weeks in complete folate-free RPMI 1640 medium plus 25 nM 5-CHO-THF. Cells were plated in medium without nucleosides, supplemented with 25 nM 5-CHO-THF, and allowed to adhere overnight. Cells were washed with DPBS and incubated in the same medium, with 25 mM PIPES/25 mM HEPES, pH 6.8, 0.06 mM adenosine, and 1 μM [^{3}H]**C1** or [^{3}H]**C2.** After 16 h, cells were washed three times with ice-cold DPBS and scraped into 5 ml of DPBS, pelleted (1500 rpm), and flash-frozen. Polyglutamyl and unmetabolized drug forms were extracted and levels were quantified by HPLC (Kugel Desmoulin et al., 2011). Cellular proteins were quantified with the Folin phenol reagent (Lowry et al., 1951). Polyglutamyl and parent drug forms were normalized to cellular proteins and are expressed as picomoles per milligram of cell protein.

In Vivo Efficacy Study of C1 and C2 in WT and R5 HeLa Xenografts. Cultured WT and R5 HeLa cells were implanted subcutaneously (~10^7 cells/flank) to establish a solid tumor xenograft model (passage 0) in female ICR SCID mice (National Institutes of Health DCT/DTP Animal Production Program, Frederick, MD). The mice were supplied food and water ad libitum. Study mice were maintained on a folate-deficient diet (TD.00434; Harlan Teklad, Madison, WI) starting 18 days before tumor implant to ensure that serum folate levels would approximate those of humans before the start of therapy (Wang et al., 2010, 2011; Kugel Desmoulin et al., 2011). This design is analogous to those previously published by others (Alati et al., 1996; Gibbs et al., 2005).

For the efficacy trial, the experimental animals were pooled, divided into groups (4 mice/group), and implanted bilaterally subcutaneously with 30- to 60-mg tumor fragments (from passage 3) using a 12-gauge trocar. Chemotherapy began on day 3 after tumor implantation, when the number of cells was between 10^7 and 10^8 cells (below the limit of palpation). An organic solvent (ethanol, 5% v/v), carrier (Tween 80, 1% v/v), and sodium bicarbonate (0.5% v/v) were used to effect solubilization of **C1** and **C2.** Injection volumes were 0.2 ml i.v. Tumors were measured with a caliper two to three times weekly. Mice were sacrificed when cumulative tumor burdens reached 1500 mg. Methods of protocol design, drug treatments, toxicity evaluation, and data analysis were described previously (Corbett et al., 1997, 1998; Polin et al., 1997, 2011). Experimental parameters as qualitative and quantitative end points to assess antitumor activities include T/C as a percentage (see legend to Table 1 for further details) and T − C (tumor growth delay) [where T is the median time in days required for the treatment group tumors to reach a predetermined size (e.g., 1000 mg) and C is the median time in days for the control group tumors to reach the same size; tumor-free survivors are excluded from these calculations] and tumor cell kill [$\log_{10}$ cell kill total (gross) = (T − C)/(3.32)(Td), where (T − C) is the tumor growth delay, as described above, and Td is the tumor volume doubling time in days, estimated from the best fit straight line from a log-linear growth plot of control group tumors in exponential growth (100–800 mg)]. The day of tumor implant was day 0. For comparison of antitumor activities with standard agents or between tumors, $\log_{10}$ kill values were converted to an arbitrary activity rating (Corbett et al., 1997). With the exception of the xenograft model, these methods are essentially identical to those described previously (Wang et al., 2010, 2011; Kugel Desmoulin et al., 2011).

Statistical Analysis. Statistical analyses were performed with GraphPad Instat 4.0.

Results

Expression and Function of hRFC and hPCFT in Human Solid Tumor Cell Lines. We previously measured substantial levels of hPCFT transcripts by real-time RT-PCR in 52 of 53 human solid tumor cell lines of different origins (e.g., breast, prostate, ovarian, and others) (Kugel Desmoulin et al., 2011). As an extension of this work, we measured levels of hPCFT proteins for 10 of the tumor cell lines (HepG2, Hep3B, H596, CRL5810, H2595, HCT15, Caco-2, DU145, MDA-MB 321, and SK-MEL5) (Supplemental Table 2S). We also analyzed four HeLa sublines, including WT and hRFC-

null R5 cells, both of which express hPCFT, and two HeLa sublines derived from hRFC- and hPCFT-null R1-11 cells including R1-11-mock (hereafter, R1-11) and R1-11-PCFT4 (R1-11 cells stably transfected with hPCFT) cells. For each cell line, plasma membrane proteins were separated by SDS-PAGE and immunoblotted with hPCFT-specific antibodies. Levels of heterogeneously glycosylated hPCFT proteins detected by Western blotting (Fig. 1A) paralleled those of hPCFT transcripts (Kugel Desmoulin et al., 2011). hPCFT proteins were detected in all tumor cell lines except for the parental R1-11 cells.

Functional validation of hPCFT expression in the solid tumor cell lines was established by transport assays with [^{3}H]MTX (0.5 μM, 5 min) at pH 5.5 (Fig. 1B). Substantial [^{3}H]MTX uptake at pH 5.5 was detected in cell lines expressing hPCFT protein with the highest levels in Hep3B and Caco-2, accompanying elevated PCFT protein levels.

hPCFT Transport of [^{3}H]C2 in R1-11-PCFT4 Cells. We found previously that the novel 6-substituted pyrrolo[2,3-*d*]pyrimidine thienoyl antifolates **C1** and **C2** (Fig. 2A) were potent (nanomolar) inhibitors of proliferation in cells engineered to express hPCFT in the absence of hRFC or FRs (Wang et al., 2010, 2011; Kugel Desmoulin et al., 2011), suggesting that **C1** and **C2** are substrates for hPCFT-mediated cellular uptake. In engineered cell lines, **C1** and **C2** seemed to be poorly transported by hRFC (Wang et al., 2010, 2011; Kugel Desmoulin et al., 2011). Both analogs induced current at −90 mV and pH 5.5 in *Xenopus laevis* oocytes microinjected with hPCFT cRNAs, and both were competitive inhibitors of [^{3}H]MTX transport in hPCFT transfectants from pH 5.5 to pH 6.8 (Kugel Desmoulin et al., 2011; Wang et al., 2011). Transport of [^{3}H]**C1** by hPCFT was directly demonstrated in R1-11-PCFT4 cells (Kugel Desmoulin et al., 2011).

To confirm hPCFT transport of **C2**, R1-11-PCFT4 cells were incubated with [^{3}H]**C2** (0.5 μM, 5 min, 37°C) at pH 5.5 and 6.8 in the presence and absence of unlabeled **C1** (10 μM) as a competitive inhibitor. Transport was detected at a ~4-fold higher level at pH 5.5 than at pH 6.8, and at both pHs uptake was substantially inhibited in the presence of *unlabeled* **C1** (Fig. 2B). These results establish that **C2**, like its 4-carbon chain homolog, **C1**, is a bona fide substrate for membrane transport by hPCFT. Transport kinetic parameters for **C2** with R1-11-PCFT4 cells at pH 5.5 are summarized in Supplemental Table 4S. K_t and V_{max} values for **C2** were similar to those previously reported for **C1** and PMX (Kugel Desmoulin et al., 2011).

Transport and Membrane Expression of hPCFT and hRFC in WT and R5 HeLa Sublines. Although **C1** and **C2** are not RFC transport substrates (Wang et al., 2010, 2011; Kugel Desmoulin et al., 2011), RFC levels could nonetheless have a marked impact on the antiproliferative effects of these agents, via expansion or contraction of intracellular THF cofactor pools. Thus, RFC levels or ratios of PCFT to RFC transport might effectively predict the antitumor potencies of these prototypical PCFT-targeted antifolates. This result could be further affected by varying concentrations of extracellular THF cofactors.

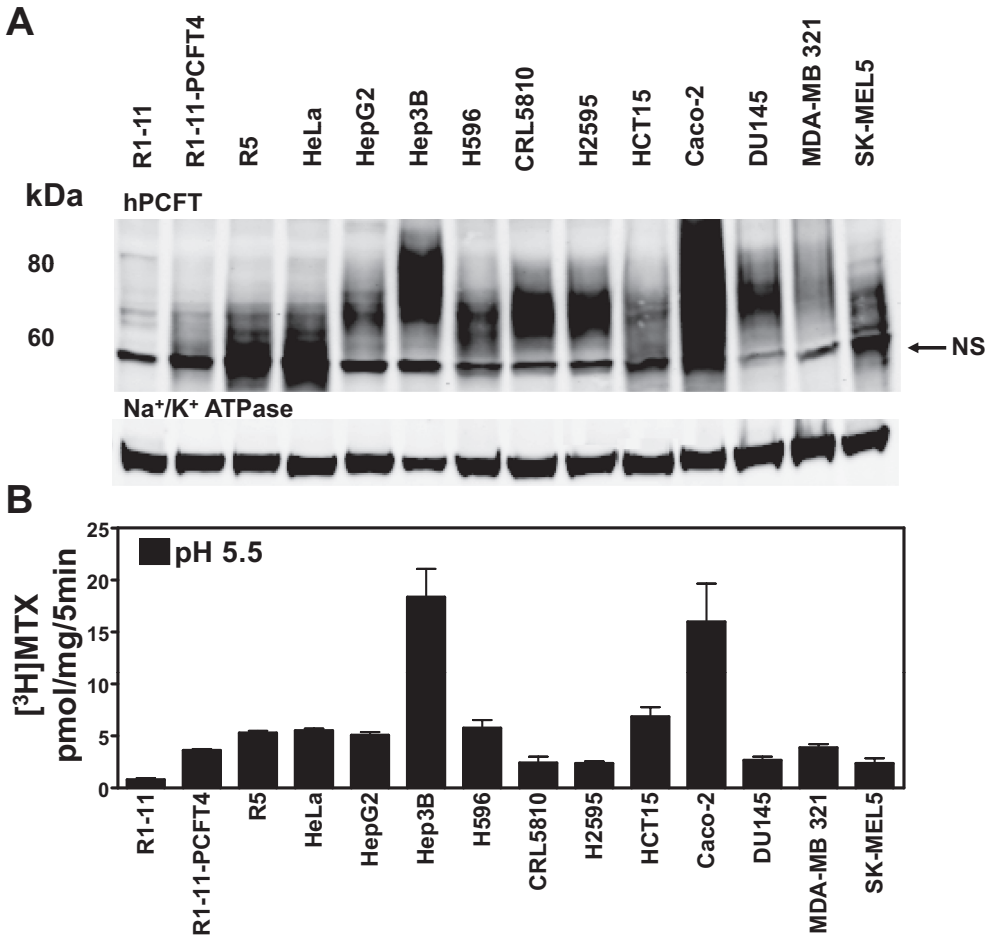

Fig. 1. PCFT expression and function in human solid tumor cell lines. A, plasma membrane preparations were isolated as described under *Materials and Methods*. Membrane proteins (25 μg) from human tumor cell lines were electrophoresed on a 7.5% denaturing polyacrylamide gel and immunoblotted with hPCFT antibody. Na^+/K^+-ATPase protein levels were used as loading controls. hPCFT migrates as a broadly banding species because of its heterogeneous glycosylation. The banding in the lane for the R1-11 HeLa cells is nonspecific. The major nonspecific band appearing in all lanes is labeled NS. B, uptake of 0.5 μM [^{3}H]MTX was measured at 37°C for 5 min in cell monolayers at pH 5.5, as described under *Materials and Methods*. Internalized [^{3}H]MTX was normalized to total protein. Results are shown for mean values ± S.E. for three to four independent experiments. The characteristics of the 14 tumor cell lines are summarized in Supplemental Table 2S.

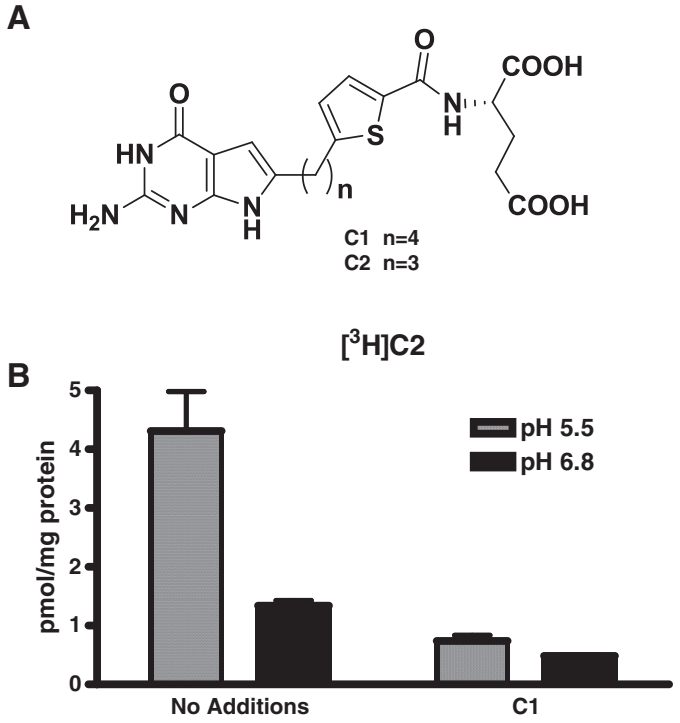

Fig. 2. PCFT transport activity of C2 in R1-11-PCFT4 HeLa cells. A, structures of 6-substituted pyrrolo[2,3-*d*]pyrimidine thienoyl antifolates **C1** and **C2** (Wang et al., 2010, 2011) are shown. B, uptake of [^{3}H]**C2** (0.5 μM) was measured at 37°C for 5 min at pH 5.5 and 6.8 in the presence or absence of unlabeled **C1** (10 μM). Internalized [^{3}H]**C2** was normalized to total protein. Details are provided under *Materials and Methods*. Results are shown for mean values ± S.E. for three independent experiments.

To explore this concept, we used WT and R5 HeLa cells, which express comparable levels of hPCFT with or without hRFC (Figs. 1 and 3A; Supplemental Fig. 1SA). R5 cells are resistant to MTX (Fig. 5A) because of a genomic deletion that results in loss of hRFC (Zhao et al., 2004a). MTX resistance is completely reversible upon transfection with WT hRFC (R5-RFC2 cells), which restores hRFC transport (Supplemental Fig. 1SB), confirming that loss of hRFC transport causes the resistant phenotype.

Whereas [^{3}H]MTX (0.5 μM) transport by hPCFT at pH 5.5 was nearly identical for WT and R5 HeLa cells (Fig. 3B), MTX uptake in R5 cells in AFB at pH 7.2 was decreased ~3-fold compared with that in WT cells (Fig. 3C), consistent with the loss of hRFC. Ratios of MTX transport at pH 5.5 (PCFT) to pH 7.2 (RFC) for R5 and WT cells were ~11 and ~3, respectively (Fig. 3D). Transport was also measured for [^{3}H]**C1** and [^{3}H]**C2** (both at 0.5 μM; 2 min, 37°C) and for [^{3}H]PMX at pH 5.5 and pH 7.2. Results were compared with those for [^{3}H]MTX (Fig. 3, B and C). For all compounds and both cell lines, transport by hPCFT over hRFC predominated, because uptake showed the characteristic pH dependence for PCFT with the highest levels at pH 5.5. Although there were slight differences in initial rates of uptake of the various analogs at pH 5.5, these were not statistically significant. Furthermore, there were no obvious differences in membrane transport of the individual analogs between WT and R5 HeLa cell lines.

Impact of hRFC and Extracellular Folate on Antitumor Activities of C1 and C2. (6*S*)-5-CHO-THF is poorly transported by PCFT at neutral pH and is less effective in supporting proliferation of PCFT-expressing cells (without RFC) than RFC-expressing cells (without PCFT) (Zhao et al., 2008). Thus, loss of hRFC in R5 cells would be predicted to contract intracellular pools of reduced folates derived from 5-CHO-THF, compared with those in WT HeLa cells (Zhao et al., 2004b; Chattopadhyay et al., 2006). This effect may be exacerbated in the presence of high-affinity hPCFT-selective substrates, which could further restrict the modest levels of THF cofactor uptake via PCFT through direct competition.

To examine these possibilities, folate-depleted WT, R5, and R5-RFC2 cells were cultured in 25, 100, or 1000 nM [^{3}H]5-CHO-THF [corresponding to 12.5, 50, or 500 nM concentrations of the active (6*S*) stereoisomer] for 96 h to determine cellular accumulations of [^{3}H]THF metabolites. During sustained culture, the media pH decreased to ~6.8 (Kugel Des-

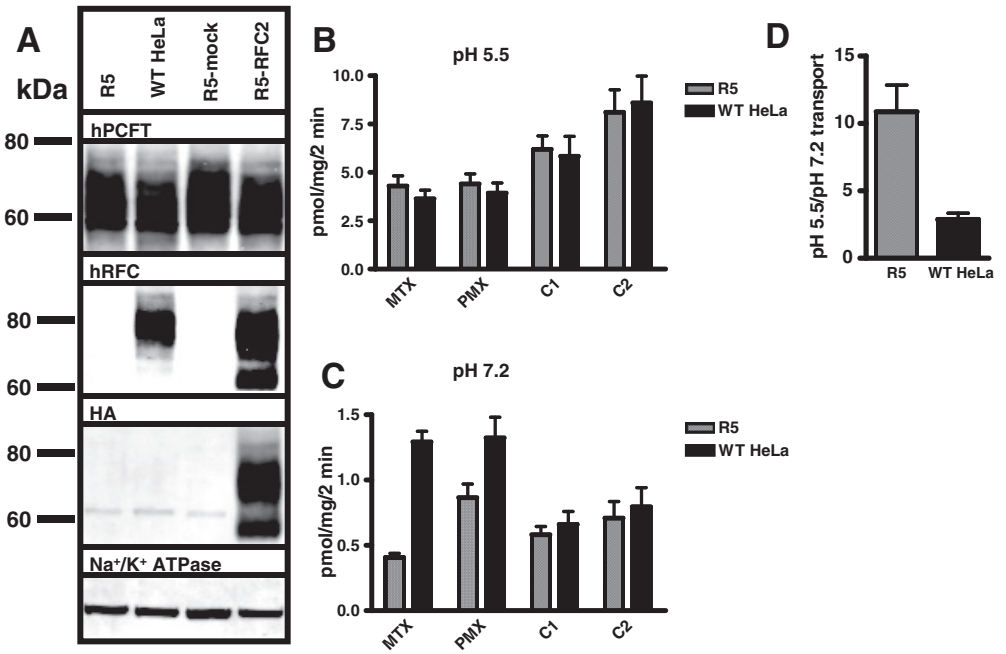

Fig. 3. Characterization of WT and R5 HeLa sublines. A, representative Western blots are shown for sucrose gradient-purified membrane fractions (25 μg) using hPCFT, hRFC, and HA antibodies to detect WT and HA-tagged (R5-RFC^{HA}) proteins. Uptakes of 0.5 μM [^{3}H]MTX, [^{3}H]PMX, [^{3}H]**C1,** and [^{3}H]**C2** were measured at 37°C for 2 min in WT and R5 HeLa cell monolayers at pH 5.5 (B) and pH 7.2 (C). Internalized tritiated drug was normalized to total cellular protein. Experimental details are provided under *Materials and Methods*. D, ratios of [^{3}H]MTX uptake at pH 5.5/pH 7.2 in WT and R5 HeLa cells are plotted. The data in B to D represent mean values ± S.E. for three independent experiments. Although there were slight differences in initial rates of uptake for **C1** and **C2** for both WT and R5 HeLa cells in B, these were not statistically significant ($p > 0.1$), consistent with the very modest differences in transport kinetics between these drugs (Supplemental Table 4S).

moulin et al., 2010) and was accompanied by dose-dependent accumulations of [^{3}H]5-CHO-THF (Fig. 4A). At 25 nM [^{3}H]5-CHO-THF, R5 cells experienced a 31.6% decreased net accumulation of tritiated folates compared with that in WT cells ($p < 0.05$) and a 49.6% decrease compared with that in R5-RFC2 cells ($p < 0.05$). Whereas this difference between WT and R5 cells decreased at 100 and 1000 nM [^{3}H]5-CHO-THF, statistically significant differences in [^{3}H]5-CHO-THF accumulations were preserved at these concentrations between R5 and R5-RFC2 cells (Fig. 4A).

We measured proliferation of WT and R5 HeLa cells grown in 25 nM 5-CHO-THF in the presence of a range of concentrations (0–1000 nM) of the PCFT-selective antifolates **C1** and **C2** for comparison with MTX, lometrexol (LMX), raltitrexed (RTX), and PMX, classic antifolates that are transported by both RFC and PCFT (Goldman et al., 2010; Kugel Desmoulin et al., 2010, 2011) and with N^{α}-(4-amino-4-deoxypteroyl)-N^{δ}-hemiphthaloyl-L-ornithine (PT523), which is transported by RFC but not by PCFT (Zhao and Goldman, 2007; Kugel Desmoulin et al., 2010, 2011) (Fig. 5A; Supplemental Table 5S). Similar to published results (Zhao et al., 2004c), R5 (and R5-mock transfected) cells were substantially resistant to PT523 compared with WT (> 213-fold) and R5-RFC2 (> 303-fold) cells. Furthermore, R5 cells were resistant (5- to 14-fold) to MTX, LMX, and RTX compared with WT HeLa cells. For PMX, IC_{50} values for WT and R5 cells were modestly different (IC_{50} values of 48.3 and 66.1 nM, respectively). It is noteworthy that hRFC-deficient R5 cells were substantially *more sensitive* to the PCFT-specific antifolates **C1** and **C2** than were WT cells (3.6- and 3.2-fold, respectively) and R5-RFC2 transfected cells (3.6- and 8.3-fold, respectively). Although differences in growth inhibitions between R5 and WT cells for **C1** and **C2** were preserved when the extracellular 5-CHO-THF was increased to 100 nM (4.3- and 15-fold, respectively), the effects of both drugs were effectively abolished when the 5-CHO-THF concentration was increased to 1000 nM (Fig. 5, B and C).

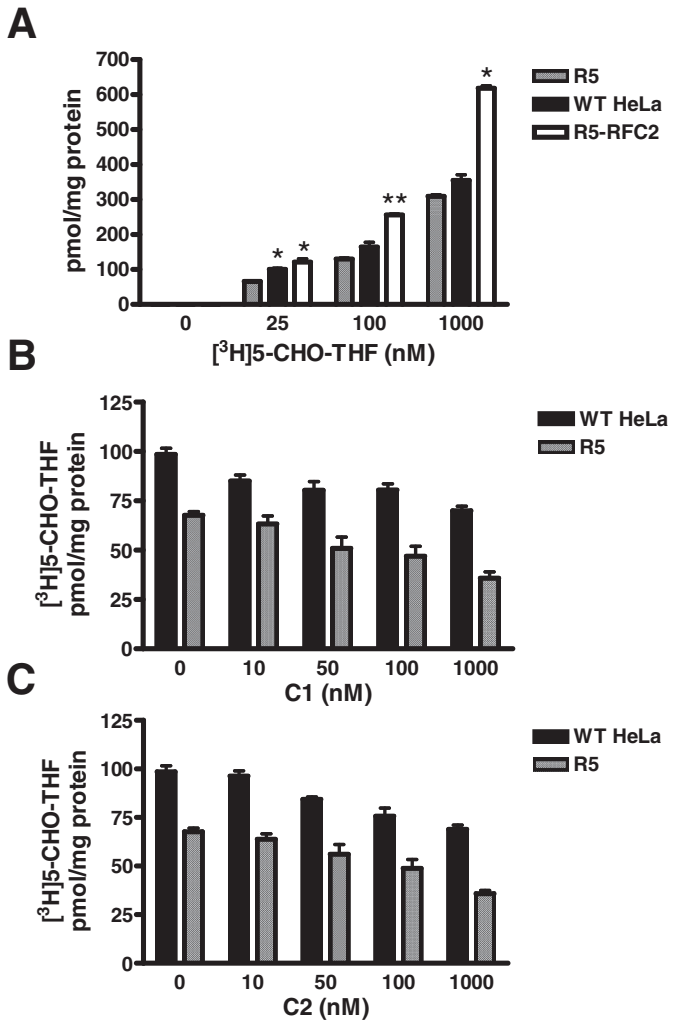

Fig. 4. [^{3}H]5-CHO-THF accumulations in WT and R5 HeLa sublines. Folate-depleted R5 HeLa sublines were treated for 96 h with increasing concentrations of [^{3}H]5-CHO-THF (0–1000 nM) (A) or with 25 nM [^{3}H]5-CHO-THF and 0 to 1000 nM unlabeled **C1** (B) or **C2** (C). Internalized [^{3}H]5-CHO-THF was normalized to total cellular proteins. Details are described under *Materials and Methods*. The data in A summarize the results as mean values ± S.E. for three independent experiments. For each 5-CHO-THF concentration, statistically significant differences were calculated between WT or R5-RFC2 cells and R5 cells: *, $p < 0.05$; **, $p < 0.005$. B and C, both R5 and WT HeLa cells showed decreased total folate metabolites derived from [^{3}H]5-CHO-THF, accompanying treatment with increased concentrations of **C1** or **C2** (results are mean values ± S.E. for three to five independent experiments). The decreases between untreated controls and 1000 nM antifolate treatments were greater for R5 cells than for WT HeLa cells with both **C1** (decreased 47.1 and 28.1%, respectively; $p = 0.006$) and **C2** (decreased 47.3 and 29.1%, respectively; $p = 0.078$).

Because **C1** and **C2** are high-affinity substrates for PCFT, we hypothesized that these drugs compete with [^{3}H]5-CHO-THF for PCFT uptake, leading to a more severe contraction of the cellular folate pool in R5 cells compared with WT cells than in their absence. Indeed, both **C1** and **C2** effected a striking dose-dependent decrease in net accumulations of [^{3}H]5-CHO-THF, which were greater in hRFC-null R5 cells than in WT HeLa cells. At 1000 nM **C1**, levels of [^{3}H]5-CHO-THF accumulation in R5 and WT HeLa cells were 52.9 and 72.9%, respectively, of levels without drug; for **C2**, the corresponding values were 52.7 and 71.1%, respectively (Fig. 4, B and C).

Collectively, these results establish that loss of hRFC contributes to a contraction of cellular folate pools, which is exacerbated in the presence of the PCFT-selective analogs **C1** and **C2**. Of importance, decreased intracellular folates were accompanied by markedly increased antiproliferative effects of **C1** and **C2**.

Polyglutamylation of C1 and C2 in WT and R5 HeLa Cells. Analogous to physiologic folates and other classic antifolate drugs such as MTX (Goldman and Matherly, 1985; Shane, 1989; Assaraf, 2007), **C1** is metabolized to polyglutamates (PGs) (Kugel Desmoulin et al., 2011). Polyglutamylation of **C2** has not been assessed previously. Because polyglutamylation of antifolate drugs by folylpolyglutamate synthetase (FPGS) can be regulated by elevated extra- and intracellular folates (Tse and Moran, 1998; Zhao et al., 2001), it seemed possible that the impact of hRFC and cellular THF cofactors on the antiproliferative effects of **C1** and **C2** may be partly explained in this manner.

To assess this possibility, WT and R5 HeLa cells were incubated with 1 μM [^{3}H]**C1** or [^{3}H]**C2** for 16 h at pH 6.8 in the presence of 25 nM 5-CHO-THF and 0.06 mM adenosine. Total cellular radiolabeled drug levels were quantified, and tritiated parent drug and PGs were extracted and analyzed. At least four polyglutamyl metabolites (PG_{2-5}) of [^{3}H]**C1** and five metabolites of [^{3}H]**C2** (PG_{2-6}) were resolved by HPLC. Migrations were compared with those for nonpolyglutamyl

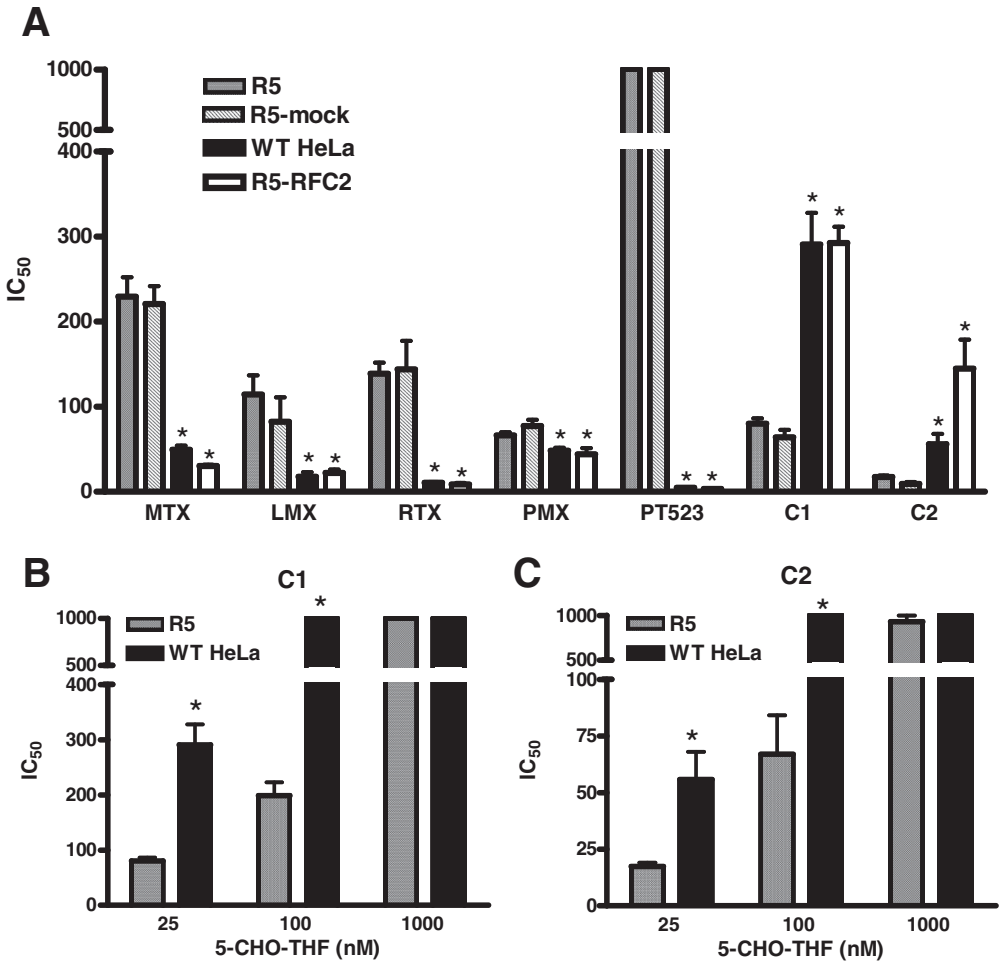

Fig. 5. Growth inhibition by antifolate drugs toward WT and R5 HeLa sublines. A, growth inhibitions were measured by a fluorescence (CellTiter-Blue)-based assay after 96 h of exposure of WT, R5, R5-mock, and R5-RFC2 HeLa sublines to a range of inhibitor concentrations. Results are presented as mean IC_{50} values ± S.E. from 5 to 12 independent experiments. IC_{50} values are summarized in Supplemental Table 5S. Statistically significant differences between results for WT HeLa or R5-RFC2 cells and those for R5 cells: *, $p < 0.01$. For **C1** (B) and **C2** (C), growth inhibition experiments were performed in the presence of increasing concentrations (25, 100, and 1000 nM) of extracellular 5-CHO-THF. Results are summarized as mean IC_{50} values ± S.E. from 3 to 11 independent experiments. Statistically significant differences between results for WT HeLa and those for R5 HeLa cells: *, $p < 0.005$.

C1 or **C2** and with MTX and MTX PG standards. Furthermore, samples were treated in parallel with conjugase (Kugel Desmoulin et al., 2011), which reverted the majority of the polyglutamyl metabolites to the parental drugs (not shown). Results are summarized in Supplemental Fig. 2S. HPLC chromatograms for the radiolabeled drug forms in HeLa and R5 cells are shown in Supplemental Fig. 3S. For R5 and WT cells, there was a 7- to 8-fold greater accumulation of total and polyglutamyl [^{3}H]**C2** than for [^{3}H]**C1**. WT and R5 cells accumulated similar levels of total **C1** and **C2** drug forms, although there were slight differences in relative accumulations of individual PGs between the cell lines. This difference was most obvious for the longest chain length PGs (PG_5 and PG_6) and was somewhat greater for **C1** than for **C2**.

These results establish that 1) both **C1** and **C2** are excellent substrates for polyglutamylation under conditions that favor their membrane transport by PCFT, 2) net drug accumulation and polyglutamylation of **C2** far exceeds that for **C1,** and 3) the presence or absence of functional RFC manifests at most a modest effect on net **C1** and **C2** polyglutamate synthesis.

In Vivo Efficacy of C1 and C2 against WT and R5 HeLa Xenografts. To extend our in vitro cell proliferation studies in vivo, we performed in vivo antitumor efficacy studies with 8-week-old female ICR SCID mice implanted with subcutaneous R5 or WT HeLa cells. Mice were maintained ad libitum on a folate-deficient diet, which decreased serum folates to levels approximating those seen in humans. For the efficacy trial, control and drug treatment groups were non-selectively randomized (four mice/group); **C1** or **C2** was administered intravenously (180 and 32 mg/kg per injection, respectively) on days 3, 7, 14, and 18 after implantation. As reported for other tumor models (Kugel Desmoulin et al., 2011; Wang et al., 2011), **C1** and **C2** showed substantial efficacies toward R5 and WT HeLa xenografts (Table 1). Both **C1** and **C2** showed greater efficacies toward R5 cells (T − C = 23 days, 3.3 gross $\log_{10}$ kill for **C1**; T − C = 17.5 days, 2.5 gross $\log_{10}$ kill for **C2**) than toward WT cells (T − C = 13 days, 1.9 gross $\log_{10}$ kill for **C1**; T − C = 13 days, 1.9 gross $\log_{10}$ kill for **C2**). Differences in C − T and $\log_{10}$ kill results between R5 and WT HeLa cells for compound **C1** were statistically significant ($p = 0.014$ and $p = 0.0135$, respectively). However, differences in these parameters for **C2** did not quite reach statistical significance ($p = 0.146$). The treatment regimens with **C1** and **C2** were well tolerated with dose-limiting symptoms manifesting as reversible body weight loss.

The results of the in vivo efficacy trial provide proof-of-principle confirmation of our in vitro findings that the antitumor effects of both **C1** and **C2** are greater in hRFC-deficient R5 cells than in WT cells. Of interest, the impact of loss of hRFC seems to be somewhat greater with **C1** than with **C2** in vivo.

Discussion

In this study, we expanded on previous reports (Zhao and Goldman, 2007; Goldman et al., 2010; Kugel Desmoulin et al., 2010, 2011; Wang et al., 2010, 2011) that hPCFT may be

TABLE 1

Antitumor efficacy evaluation of **C1** and **C2** against early-stage human R5 and HeLa in female SCID mice

The 8-week-old female NCR SCID mice were implanted bilaterally subcutaneously with 30- to 60-mg tumor fragments by a 12-gauge trocar on day 0. Both tumor studies (WT and R5 HeLa cells) used four mice per group. Median mouse body weights for each experiment were within 2 g and were 19 g (WT) or 19.5 g (R5) HeLa cells at the start of therapy. Chemotherapy was started on day 3 after tumor implantation, when the numbers of cells were small (10^7–10^8 cells). Day 0 is the day of tumor implant. Median tumor masses were determined (including zeros). To determine the T/C value, the treatment and control groups were measured when the control group tumors reached 1000 mg in size (median of group). T/C is an indication of antitumor effectiveness. T/C ≤42% is considered significant antitumor activity by the Drug Evaluation Branch of the Division of Cancer Treatment (National Cancer Institute). T/C <10% is considered to indicate highly significant antitumor activity and is the level used to justify a clinical trial if toxicity, formulation, and certain other requirements are met. T/C = 0 indicates very high antitumor activity. Statistical analyses were performed for the differences in T − C and $\log_{10}$ kills between WT and R5 HeLa cells for **C1** and **C2** relative to the median control values for each tumor. Differences in T − C and $\log_{10}$ kill results between R5 and WT HeLa cells for compound **C1** were statistically significant ($P = 0.014$ and $P = 0.0135$, respectively). Whereas these parameters also differed for **C2** between the cell lines, these differences did not quite reach statistical significance ($P = 0.146$).

Tumor and Agent	Total Dose	Median (Range) Tumor Mass on Day 21	T/C (%)	Time (Range) to 1000 mg	T − C	Gross $\log_{10}$ Kill	Activity Rating
	mg/kg	*mg*	*%*	*days*			
R5							
No treatment		1054 (916–1272)		21 (20–22)			−
C1	720	0 (all zeros)	0	44 (39–49)	23	3.3	++++
C2	128	32 (0–75)	3	38.5 (36–42)	17.5	2.5	+++
HeLa							
No treatment		1009 (847–1701)		21 (18–22)			−
C1	720	63 (0–247)	6	34 (31–37)	13	1.9	++
C2	128	69 (0–189)	7	34 (30–40)	13	1.9	++

++++, >2.8 log10 kill, highly active; +++, 2.0 to 2.8; ++, 1.3 to 1.9; and −, <0.7, inactive.

exploitable for cancer therapy, reflecting unique patterns of hPCFT expression and appreciable transport activity at pH values approximating the tumor microenvironment. We extended our previous findings establishing broad-ranging hPCFT gene expression in a large number of human tumor cell lines (Kugel Desmoulin et al., 2011) to include measurements of hPCFT protein and transport activity. Our results document the fact that hPCFT protein levels are abundantly expressed, accompanying substantial transport activities at pH 5.5.

We demonstrated that functional loss of hRFC in R5 cells caused a contraction of total cellular THF cofactor pools derived from 5-CHO-THF, which enhanced both **C1** and **C2** antitumor activities compared with those in WT cells. Of importance, the reduction in total cellular folate pools in R5 cells was exacerbated in the presence of **C1** and **C2**, through direct competition at hPCFT, which further restricted cellular uptake of exogenous 5-CHO-THF. Efficacies of **C1** and **C2** toward R5 tumors were also increased compared with those toward WT tumors transplanted into SCID mice with serum folate concentrations approximating those achieved in humans, although this effect seemed to be somewhat greater with **C1** than with **C2** in vivo. We previously reported that the in vivo efficacy of **C2** toward IGROV1 xenografts in SCID mice was less affected by serum folates than that for **C1** (Wang et al., 2010, 2011).

There is ample precedent for an impact of folate pools on antifolate drug efficacy. Indeed, this is the premise of leucovorin rescue from MTX toxicity (Matherly et al., 1987) and of low-dose folic acid protection from LMX toxicity in vivo (Roberts et al., 2000), whereby elevated extra- and intracellular folates compete at multiple levels to reverse drug activity. In vitro studies have extended these findings to both classic (PMX and LMX) and nonclassic (trimetrexate) antifolates, which inhibit a range of cellular targets (Tse and Moran, 1998; Zhao et al., 2001; Goldman et al., 2010). Furthermore, antifolate drug activities are enhanced by decreased intracellular folates resulting from an hRFC genomic deletion (Zhao et al., 2004b,c; Chattopadhyay et al., 2006) or hRFC mutations (Zhao et al., 2000a). Conversely, antifolate effects are reduced by increased intracellular folates resulting from impaired efflux of folic acid (Assaraf and Goldman, 1997) or enhanced folic acid influx by a mutant RFC (Tse and Moran, 1998; Tse et al., 1998).

Regardless of the underlying mechanism and intracellular drug target involved, markedly decreased total intracellular THF pools can result in collateral sensitivities to antifolates, often in the face of substantially decreased levels of drug uptake (Zhao et al., 2000b, 2001, 2004c; Chattopadhyay et al., 2006). The effects of folate levels on antifolate activities could reflect inhibitory effects on drug polyglutamylation (with consequent impact on drug retention and inhibition of folate-dependent enzyme targets) as a result of competitive feedback inhibition at FPGS by high levels of THF cofactor PGs (Nimec and Galivan, 1983; Shane, 1989; Tse and Moran, 1998; Zhao et al., 2001, 2004b) or increased FPGS activity levels in response to decreased extra- and intracellular folates (Gates et al., 1996). Furthermore, direct competitive interactions between polyglutamyl folates and antifolates may substantially interfere with drug binding and inhibition at their enzyme targets, as documented for MTX (Matherly et al., 1983). Changes in drug efflux are also possible, because ABC transporter (ABCG2, ABCC1) levels and/or intracellular distributions have been described in response to folate deprivation (Ifergan et al., 2005).

In the present study, we found that **C1** and **C2** membrane transport by PCFT was virtually identical between the hRFC-deficient R5 and WT HeLa cell lines. Total and polyglutamyl accumulations of **C1** and **C2** during sustained drug exposures were similar between WT and R5 cells, although there were slight differences in distributions of **C1** and **C2** polyglutamates between the lines. This difference was most pronounced for the longest chain length PGs (PG_5 and PG_6) and seemed to be somewhat greater for **C1** than **C2**. By analogy with other classic antifolates (Mendelsohn et al., 1999; Shih and Thornton, 1999), increased accumulation of long-chain polyglutamyl forms of **C1** and **C2** in the R5 subline might result in enhanced inhibition of intracellular glycinamide ribonucleotide formyltransferase and de novo purine nucleotide biosynthesis (Wang et al., 2010, 2011; Kugel Desmoulin et al., 2011), thus further exacerbating the impact

of reduced cellular folate pools in directly competing for binding to this enzyme target.

Our results provide proof-of-principle evidence that hRFC levels and function are critical determinants of antitumor activities and in vivo efficacies of PCFT-targeted antifolates that are not themselves RFC substrates. This lack of RFC transport confers tumor selectivity and decreased toxicity to normal tissues for this novel class of agents. Tumor selectivity would be enhanced by substantial levels of hPCFT protein in solid tumors and by acidic pH values characterizing the tumor microenvironment, which favor PCFT over RFC transport (Kugel Desmoulin et al., 2011). Conversely, at neutral pH values characterizing most normal tissues, RFC transport of reduced folates would be increased, resulting in elevated levels of THF cofactors within cells, which further protect from untoward drug effects. Of course, as suggested in this report, in tumors with sufficiently high hRFC, uptake of THF cofactors by this process will probably occur, even at somewhat acidic pH values. Accordingly, any decrease in hRFC function would serve to augment the inherent antitumor selectivities and increase sensitivities to PCFT-selective antifolates.

Acknowledgments

We thank Dr. I. David Goldman for his generous gifts of the R5 and R1-11 HeLa cell lines. We thank Kelly Haagenson for editorial assistance.

Authorship Contributions

Participated in research design: Kugel Desmoulin, Wang, Polin, Hou, Gangjee, and Matherly.

Conducted experiments: Kugel Desmoulin, Wang, Polin, White, Kushner, Stout, Hou, and Cherian.

Performed data analysis: Kugel Desmoulin, Wang, Polin, Stout, Hou, Gangjee, and Matherly.

Wrote or contributed to the writing of the manuscript: Kugel Desmoulin, Polin, Hou, Gangjee, and Matherly.

References

Alati T, Worzalla JF, Shih C, Bewley JR, Lewis S, Moran RG, and Grindey GB (1996) Augmentation of the therapeutic activity of lometrexol-(6-*R*)5,10-dideazatetrahydrofolate- by oral folic acid. *Cancer Res* **56:**2331–2335.

Anderson CM and Thwaites DT (2010) Hijacking solute carriers for proton-coupled drug transport. *Physiology* (*Bethesda*) **25:**364–377.

Assaraf YG (2007) Molecular basis of antifolate resistance. *Cancer Metastasis Rev* **26:**153–181.

Assaraf YG and Goldman ID (1997) Loss of folic acid exporter function with markedly augmented folate accumulation in lipophilic antifolate-resistant mammalian cells. *J Biol Chem* **272:**17460–17466.

Chattopadhyay S, Moran RG, and Goldman ID (2007) Pemetrexed: biochemical and cellular pharmacology, mechanisms, and clinical applications. *Mol Cancer Ther* **6:**404–417.

Chattopadhyay S, Zhao R, Krupenko SA, Krupenko N, and Goldman ID (2006) The inverse relationship between reduced folate carrier function and pemetrexed activity in a human colon cancer cell line. *Mol Cancer Ther* **5:**438–449.

Corbett TH, LoRusso P, Demchick L, Simpson C, Pugh S, White K, Kushner J, Polin L, Meyer J, Czarnecki J, et al. (1998) Preclinical antitumor efficacy of analogs of XK469: sodium-(2-[4-(7-chloro-2-quinoxalinyloxy)phenoxy]propionate. *Invest New Drugs* **16:**129–139.

Corbett TH, Valeriote FA, Demchik L, Lowichik N, Polin L, Panchapor C, Pugh S, White K, Kushner J, Rake J, et al. (1997) Discovery of cryptophycin-1 and BCN-183577: examples of strategies and problems in the detection of antitumor activity in mice. *Invest New Drugs* **15:**207–218.

Gates SB, Worzalla JF, Shih C, Grindey GB, and Mendelsohn LG (1996) Dietary folate and folylpolyglutamate synthetase activity in normal and neoplastic murine tissues and human tumor xenografts. *Biochem Pharmacol* **52:**1477–1479.

Ge Y, Haska CL, LaFiura K, Devidas M, Linda SB, Liu M, Thomas R, Taub JW, and Matherly LH (2007) Prognostic role of the reduced folate carrier, the major membrane transporter for methotrexate, in childhood acute lymphoblastic leukemia: a report from the Children's Oncology Group. *Clin Cancer Res* **13:**451–457.

Gibbs DD, Theti DS, Wood N, Green M, Raynaud F, Valenti M, Forster MD, Mitchell F, Bavetsias V, Henderson E, et al. (2005) BGC 945, a novel tumor-selective thymidylate synthase inhibitor targeted to α-folate receptor-overexpressing tumors. *Cancer Res* **65:**11721–11728.

Gillies RJ, Raghunand N, Karczmar GS, and Bhujwalla ZM (2002) MRI of the tumor microenvironment. *J Magn Reson Imaging* **16:**430–450.

Goldman ID, Chattopadhyay S, Zhao R, and Moran R (2010) The antifolates: evolution, new agents in the clinic, and how targeting delivery via specific membrane transporters is driving the development of a next generation of folate analogs. *Curr Opin Investig Drugs* **11:**1409–1423.

Goldman ID and Matherly LH (1985) The cellular pharmacology of methotrexate. *Pharmacol Ther* **28:**77–102.

Gorlick R, Goker E, Trippett T, Steinherz P, Elisseyeff Y, Mazumdar M, Flintoff WF, and Bertino JR (1997) Defective transport is a common mechanism of acquired methotrexate resistance in acute lymphocytic leukemia and is associated with decreased reduced folate carrier expression. *Blood* **89:**1013–1018.

Guo W, Healey JH, Meyers PA, Ladanyi M, Huvos AG, Bertino JR, and Gorlick R (1999) Mechanisms of methotrexate resistance in osteosarcoma. *Clin Cancer Res* **5:**621–627.

Helmlinger G, Yuan F, Dellian M, and Jain RK (1997) Interstitial pH and pO_2 gradients in solid tumors in vivo: high-resolution measurements reveal a lack of correlation. *Nat Med* **3:**177–182.

Hou Z, Kugel Desmoulin S, Etnyre E, Olive M, Hsiung B, Cherian C, Wloszczynski PA, Moin K, and Matherly LH (2012) Identification and functional impact of homo-oligomers of the human proton-coupled folate transporter. *J Biol Chem* **287:**4982–4995.

Ifergan I, Jansen G, and Assaraf YG (2005) Cytoplasmic confinement of breast cancer resistance protein (BCRP/ABCG2) as a novel mechanism of adaptation to short-term folate deprivation. *Mol Pharmacol* **67:**1349–1359.

Kugel Desmoulin S, Wang L, Hales E, Polin L, White K, Kushner J, Stout M, Hou Z, Cherian C, Gangjee A, et al. (2011) Therapeutic targeting of a novel 6-substituted pyrrolo [2,3-*d*]pyrimidine thienoyl antifolate to human solid tumors based on selective uptake by the proton-coupled folate transporter. *Mol Pharmacol* **80:**1096–1107.

Kugel Desmoulin S, Wang Y, Wu J, Stout M, Hou Z, Fulterer A, Chang MH, Romero MF, Cherian C, Gangjee A, et al. (2010) Targeting the proton-coupled folate transporter for selective delivery of 6-substituted pyrrolo[2,3-*d*]pyrimidine antifolate inhibitors of de novo purine biosynthesis in the chemotherapy of solid tumors. *Mol Pharmacol* **78:**577–587.

Laemmli UK (1970) Cleavage of structural proteins during the assembly of the head of bacteriophage T4. *Nature* **227:**680–685.

Lowry OH, Rosebrough NJ, Farr AL, and Randall RJ (1951) Protein measurement with the Folin phenol reagent. *J Biol Chem* **193:**265–275.

Matherly LH, Barlowe CK, Phillips VM, and Goldman ID (1987) The effects on 4-aminoantifolates on 5-formyltetrahydrofolate metabolism in L1210 cells. A biochemical basis of the selectivity of leucovorin rescue. *J Biol Chem* **262:**710–717.

Matherly LH, Czajkowski CA, and Angeles SM (1991) Identification of a highly glycosylated methotrexate membrane carrier in K562 human erythroleukemia cells up-regulated for tetrahydrofolate cofactor and methotrexate transport. *Cancer Res* **51:**3420–3426.

Matherly LH, Fry DW, and Goldman ID (1983) Role of methotrexate polyglutamylation and cellular energy metabolism in inhibition of methotrexate binding to dihydrofolate reductase by 5-formyltetrahydrofolate in Ehrlich ascites tumor cells in vitro. *Cancer Res* **43:**2694–2699.

Matherly LH, Hou Z, and Deng Y (2007) Human reduced folate carrier: translation of basic biology to cancer etiology and therapy. *Cancer Metastasis Rev* **26:**111–128.

Matsudaira P (1987) Sequence from picomole quantities of proteins electroblotted onto polyvinylidene difluoride membranes. *J Biol Chem* **262:**10035–10038.

Mendelsohn LG, Worzalla JF, and Walling JM (1999) Preclinical and clinical evaluation of the glycinamide ribonucleotide formyltransferase inhibitors lometrexol and LY309887, in *Anticancer Drug Development Guide: Antifolate Drugs in Cancer Therapy* (Jackman AL ed) pp 261–280, Humana Press, Inc., Totowa, NJ.

Nimec Z and Galivan J (1983) Regulatory aspects of the glutamylation of methotrexate in cultured hepatoma cells. *Arch Biochem Biophys* **226:**671–680.

Polin L, Corbett TH, Roberts BJ, Lawson AJ, Leopold WR, White K, Kushner J, Hazeldine S, Moore R, Rake J, and Horwitz JP (2011) transplantable syngeneic rodent tumors: solid tumors, in *Mice Tumor Models in Cancer Research* (Teicher BA ed) pp 43–78, Humana Press, Inc., Totowa, NJ.

Polin L, Valeriote F, White K, Panchapor C, Pugh S, Knight J, LoRusso P, Hussain M, Liversidge E, Peltier N, et al. (1997) Treatment of human prostate tumors PC-3 and TSU-PR1 with standard and investigational agents in SCID mice. *Invest New Drugs* **15:**99–108.

Qiu A, Jansen M, Sakaris A, Min SH, Chattopadhyay S, Tsai E, Sandoval C, Zhao R, Akabas MH, and Goldman ID (2006) Identification of an intestinal folate transporter and the molecular basis for hereditary folate malabsorption. *Cell* **127:**917–928.

Roberts JD, Poplin EA, Tombes MB, Kyle B, Spicer DV, Grant S, Synold T, and Moran R (2000) Weekly lometrexol with daily oral folic acid is appropriate for phase II evaluation. *Cancer Chemother Pharmacol* **45:**103–110.

Shane B (1989) Folylpolyglutamate synthesis and role in the regulation of one-carbon metabolism. *Vitam Horm* **45:**263–335.

Shih C and Thornton DE (1999) Preclinical pharmacology studies and the clinical development of a novel multitargeted antifolate, MTA (LY231514), in *Anticancer Drug Development Guide: Antifolate Drugs in Cancer Therapy* (Jackman AL ed) pp 183–201, Humana Press, Inc., Totowa, NJ.

Sirotnak FM, Moccio DM, Kelleher LE, and Goutas LJ (1981) Relative frequency and kinetic properties of transport-defective phenotypes among methotrexate-resistant L1210 clonal cell lines derived in vivo. *Cancer Res* **41:**4447–4452.

Tse A, Brigle K, Taylor SM, and Moran RG (1998) Mutations in the reduced folate carrier gene which confer dominant resistance to 5,10-dideazatetrahydrofolate. *J Biol Chem* **273:**25953–25960.

Tse A and Moran RG (1998) Cellular folates prevent polyglutamation of 5,10-

dideazatetrahydrofolate. A novel mechanism of resistance to folate antimetabolites. *J Biol Chem* **273:**25944–25952.
Umapathy NS, Gnana-Prakasam JP, Martin PM, Mysona B, Dun Y, Smith SB, Ganapathy V, and Prasad PD (2007) Cloning and functional characterization of the proton-coupled electrogenic folate transporter and analysis of its expression in retinal cell types. *Invest Ophthalmol Vis Sci* **48:**5299–5305.
Wang L, Cherian C, Desmoulin SK, Polin L, Deng Y, Wu J, Hou Z, White K, Kushner J, Matherly LH, et al. (2010) Synthesis and antitumor activity of a novel series of 6-substituted pyrrolo[2,3-*d*]pyrimidine thienoyl antifolate inhibitors of purine biosynthesis with selectivity for high affinity folate receptors and the proton-coupled folate transporter over the reduced folate carrier for cellular entry. *J Med Chem* **53:**1306–1318.
Wang L, Desmoulin SK, Cherian C, Polin L, White K, Kushner J, Fulterer A, Chang MH, Mitchell-Ryan S, Stout M, et al. (2011) Synthesis, biological, and antitumor activity of a highly potent 6-substituted pyrrolo[2,3-*d*]pyrimidine thienoyl antifolate inhibitor with proton-coupled folate transporter and folate receptor selectivity over the reduced folate carrier that inhibits β-glycinamide ribonucleotide formyltransferase. *J Med Chem* **54:**7150–7164.
Webb BA, Chimenti M, Jacobson MP, and Barber DL (2011) Dysregulated pH: a perfect storm for cancer progression. *Nat Rev Cancer* **11:**671–677.
Wong SC, McQuade R, Proefke SA, Bhushan A, and Matherly LH (1997) Human K562 transfectants expressing high levels of reduced folate carrier but exhibiting low transport activity. *Biochem Pharmacol* **53:**199–206.
Wong SC, Zhang L, Proefke SA, Hukku B, and Matherly LH (1998) Gene amplification and increased expression of the reduced folate carrier in transport elevated K562 cells. *Biochem Pharmacol* **55:**1135–1138.
Yang R, Sowers R, Mazza B, Healey JH, Huvos A, Grier H, Bernstein M, Beardsley GP, Krailo MD, Devidas M, et al. (2003) Sequence alterations in the reduced folate carrier are observed in osteosarcoma tumor samples. *Clin Cancer Res* **9:**837–844.
Zhao R, Babani S, Gao F, Liu L, and Goldman ID (2000a) The mechanism of transport of the multitargeted antifolate (MTA) and its cross-resistance pattern in cells with markedly impaired transport of methotrexate. *Clin Cancer Res* **6:**3687–3695.
Zhao R, Chattopadhyay S, Hanscom M, and Goldman ID (2004a) Antifolate resistance in a HeLa cell line associated with impaired transport independent of the reduced folate carrier. *Clin Cancer Res* **10:**8735–8742.
Zhao R, Gao F, Babani S, and Goldman ID (2000b) Sensitivity to 5,10-dideazatetrahydrofolate is fully conserved in a murine leukemia cell line highly resistant to methotrexate due to impaired transport mediated by the reduced folate carrier. *Clin Cancer Res* **6:**3304–3311.
Zhao R, Gao F, and Goldman ID (2001) Marked suppression of the activity of some, but not all, antifolate compounds by augmentation of folate cofactor pools within tumor cells. *Biochem Pharmacol* **61:**857–865.
Zhao R, Gao F, Hanscom M, and Goldman ID (2004b) A prominent low-pH methotrexate transport activity in human solid tumors: contribution to the preservation of methotrexate pharmacologic activity in HeLa cells lacking the reduced folate carrier. *Clin Cancer Res* **10:**718–727.
Zhao R and Goldman ID (2003) Resistance to antifolates. *Oncogene* **22:**7431–7457.
Zhao R and Goldman ID (2007) The molecular identity and characterization of a proton-coupled folate transporter—PCFT; biological ramifications and impact on the activity of pemetrexed. *Cancer Metastasis Rev* **26:**129–139.
Zhao R, Hanscom M, Chattopadhyay S, and Goldman ID (2004c) Selective preservation of pemetrexed pharmacological activity in HeLa cells lacking the reduced folate carrier: association with the presence of a secondary transport pathway. *Cancer Res* **64:**3313–3319.
Zhao R, Qiu A, Tsai E, Jansen M, Akabas MH, and Goldman ID (2008) The proton-coupled folate transporter: impact on pemetrexed transport and on antifolates activities compared with the reduced folate carrier. *Mol Pharmacol* **74:**854–862.

Address correspondence to: Dr. Larry H. Matherly, Barbara Ann Karmanos Cancer Institute, 110 E. Warren Ave., Detroit, MI 48201. E-mail: matherly@karmanos.org